

Addressing Membership Inference Attack in Federated Learning with Model Compression

Gergely Dániel Németh^{a,*}, Miguel Ángel Lozano^b, Novi Quadrianto^c and Nuria Oliver^a

^aELLIS Alicante

^bUniversity of Alicante

^cUniversity of Sussex

ORCID (Gergely Dániel Németh): <https://orcid.org/0000-0002-9737-6519>, ORCID (Miguel Ángel Lozano): <https://orcid.org/0000-0002-4757-5587>, ORCID (Novi Quadrianto): <https://orcid.org/0000-0001-8819-306X>, ORCID (Nuria Oliver): <https://orcid.org/0000-0001-5985-691X>

Abstract. Federated Learning (FL) has been proposed as a privacy-preserving solution for machine learning. However, recent works have reported that FL can leak private client data through membership inference attacks. In this paper, we show that the effectiveness of these attacks on the clients negatively correlates with the size of the client’s datasets and model complexity. Based on this finding, we study the capabilities of model-agnostic Federated Learning to preserve privacy, as it enables the use of models of varying complexity in the clients. To systematically study this topic, we first propose a taxonomy of model-agnostic FL methods according to the strategies adopted by the clients to select the sub-models from the server’s model. This taxonomy provides a framework for existing model-agnostic FL approaches and leads to the proposal of new FL methods to fill the gaps in the taxonomy. Next, we analyze the privacy-performance trade-off of all the model-agnostic FL architectures as per the proposed taxonomy when subjected to 3 different membership inference attacks on the CIFAR-10 and CIFAR-100 vision datasets. In our experiments, we find that randomness in the strategy used to select the server’s sub-model to train the clients’ models can control the clients’ privacy while keeping competitive performance on the server’s side.

1 Introduction

Deep neural networks require access to large amounts of training data to achieve competitive performance. This data dependency raises concerns regarding the safeguarding of sensitive information that might be encapsulated in the data. Federated Learning (FL) has been proposed as a potential solution to mitigate such concerns [28]. FL consists of a distributed machine learning approach that enables training models without the need to transfer the raw data from different devices or locations (clients) to a central server. In each iteration of the learning process, the server shares the parameters of the learned global model with the clients which perform local computations on their respective data to update their local parameters. Their updated model parameters are then sent back to the server, which aggregates the changes made by the clients to improve the global model.

Given that the raw data never leaves the clients and only the model parameters are shared with the central server, FL has been proposed as a privacy-preserving solution for machine learning [28]. It is particularly useful in scenarios where data is distributed across multiple devices or locations, and the data owners are reluctant to share their data due to privacy or security concerns, as it is the case in healthcare [37, 23] and finance [27, 5], or intelligent smartphone interfaces [2]. While FL aims to provide privacy-by-design by keeping the data private in the clients, recent work has shown that sensitive information about the original data can be inferred by analyzing the model parameters that are shared in the communication rounds [12, 8]. To tackle this limitation, several privacy-preserving approaches for FL have been proposed to date, including local differential privacy [13, 3] and data augmentation [18, 32].

In this paper, we first show that the effectiveness of privacy attacks —namely membership inference— on the clients in a Federated Learning architecture is negatively correlated with the client’s model complexity and dataset size. Based on this finding, we study the capabilities of model-agnostic Federated Learning to preserve privacy, as it enables the use of models of varying complexity in the clients. In model-agnostic FL, the models in the clients are not necessarily of the same type and complexity as the model in the server. Thus, it enables improving the learning efficiency and the inclusion in the federation of heterogeneous clients with different levels of computational [15, 24] and communication capabilities [6, 10, 25].

We propose a taxonomy of existing model-agnostic FL approaches according to the strategies adopted by the clients that learn smaller models to select the sub-models from the server’s model. This taxonomy provides a framework to analyze existing model-agnostic FL approaches and leads to the proposal of new FL methods to fill the gaps in the taxonomy. Next, we analyze the privacy-performance trade-off of all the model agnostic FL architectures as per the proposed taxonomy when subjected to 3 different membership inference attacks on the CIFAR-10, and CIFAR-100 vision datasets. In our experiments, we find that randomness in the strategy used to select the server’s sub-model to train the clients’ models can control the clients’ privacy while keeping competitive performance on the server’s side.

The rest of the paper is structured as follows: the most relevant prior work is presented in Section 2. Section 3 describes the attacks used to measure privacy in the FL models. Section 4 reports an anal-

* Corresponding Author. Email: gergely@ellisalicante.org.

ysis of the correlation between model complexity, dataset size and privacy and motivates the use of model-agnostic frameworks for preserving privacy in FL. Our proposed taxonomy is described in Section 5. We empirically validate it and compare it with state-of-the-art methods in Section 6 and present our conclusions in Section 7.

2 Related work

In this section, we present the most relevant previous work on membership inference attacks and defenses in FL and model-agnostic FL.

On membership attacks in FL: While FL was initially motivated by the desire to preserve client data, recent studies have revealed that federated systems remain vulnerable to privacy attacks, specifically in the form of membership attacks [13, 3, 18, 32]. In our work, we focus on membership inference attacks (MIAs) [14], where the attacker’s goal is to determine whether an individual data point was part of the dataset used to train the target model. While MIAs expose less private information than other attacks, such as memorization attacks, they are still of great concern as they constitute a confidentiality violation [30]. Membership inference can also be used as a building block for mounting extraction attacks for existing machine learning as a service systems [8]. Several types of MIAs have been proposed in the literature [17, 33, 34]. In this work, we focus on black-box attacks where the attacker does not have full access to the models but is able to query them, which is a more realistic scenario than white-box attacks. Specifically, we analyze the impact of three popular attacks: Yeom [39], LiRA [9], and tMIA [26].

On MIAs defenses in FL: Differential Privacy (DP) [11] has been proposed to protect models from MIAs. One of the practical challenges of using DP is configuring the privacy parameters to strike a balance between privacy and utility. Existing analyses of privacy-preserving methods, such as DP-SGD [1] often rely on worst-case scenarios, and selecting privacy parameters solely based on theoretical results can result in a loss of utility. DP has also been found to yield significantly worse performance when training models on small datasets, such as the CIFAR-10 image dataset [19, 18]. Other methods to protect FL systems from MIAs include data augmentation to configure the privacy-accuracy trade-off with the level of noise added through augmentation [18], and early stopping [36], given that membership memorization is partially caused by overfitting [39].

On model-agnostic FL: In horizontal FL all clients use the same model architecture as the server. However, this approach can be a limitation when clients have different computational and communication capabilities. Model-agnostic FL has been proposed to address this limitation as it enables training a diversity of models in the clients according to their capacities. There are two broad types of model-agnostic FL methods: in the first category, clients leverage a public dataset to communicate via knowledge distillation, and learn completely different models without sharing a global model with the server [22, 40]. While this design enables clients to train different model architectures without limitations, its disadvantage is the lack of a competitive model in the server. In the second category, clients learn a less complex model which frequently is a smaller version of the server’s model. In this case, both the server and client-side models are trained as part of the federation [6, 10, 25]. In the context of deep neural networks, the model compression on the clients side can be achieved by training models with fewer [25] or with simpler [6, 10, 15, 21, 24] layers. Our work focuses on model-agnostic FL methods in this later category.

3 Passive black-box membership inference attacks

Attacks can occur on the client or the server-side: (1) *client* exposure or attack occurs when the attacker targets the client model, (f_c, θ_c^t) , for client $c = 1, \dots, N$ in training round $t = 1, \dots, T$. In a stateful setting [29], the attacker can collect a set of $k \leq T$ client updates $\Theta_c = \{\theta_c^{\tau_1}, \dots, \theta_c^{\tau_k}\}, \tau_i \in \{1, \dots, T\}$; (2) *server* exposure or attack takes place when the attacker is able to listen to the parameter θ^t updates that are broadcasted by the server to the clients. The attacker aims to identify the entire training dataset $\mathbb{D} = \sum_c \mathbb{D}_c$. In this paper, we consider *black-box, passive, client-side* attack on the last update sent from the client to the server θ_c^T where the attacker aims to identify instances of the client’s dataset \mathbb{D}_c for client c .

In a black-box attack, the attacker has no direct access to the model’s parameters θ_g and architecture f , but it can query the model with data instances to get the model prediction \hat{y} . The attacker’s purpose is to build an attacker model \mathcal{A} that predicts, for data instance (x, y) , if it was part of the training data \mathbb{D}_g of model $M(f, \theta_g, \mathbb{D}_g)$, where the subscript g can denote both the server and each of the clients. Passive attackers observe the behavior of a system without altering it, while active attackers engage with the system by modifying inputs or parameters to exploit vulnerabilities or extract information.

Formally, the perfect attacker’s model \mathcal{A} is given by:

$$\mathcal{A}(f, \theta_g, (x, y)) = \begin{cases} 1, & \text{if } (x, y) \in \mathbb{D}_g, M(f, \theta_g, \mathbb{D}_g) \\ 0, & \text{otherwise.} \end{cases} \quad (1)$$

We study the performance of three different black-box, membership inference attacks, described in more detail in the supplementary material (section 2).

- **Yeom attack:** In this light-weight, loss-based attack [39], the attacker chooses a global threshold ν , and selects every data instance with a loss lower than ν as a member of the training dataset.
- **LiRA attack:** In the offline version of the attack of [9], the attacker has an auxiliary dataset \mathbb{D}_a and trains shadow models $M_{sw}(f, \mathbb{D}_{sw})$ on random subsets of this dataset $\mathbb{D}_{sw} \subset \mathbb{D}_a$. The data instance is predicted to be a member of the client’s training set if the target model’s confidence score fits into the sample’s confidence score distribution in the shadow models.
- **tMIA attack:** a state-of-the-art attack that uses knowledge distillation to collect loss trajectories to identify member and non-member instances [26]. The method builds on the idea that the snapshots of the loss after each training epoch (loss trajectory) can separate the member instances from non-members better than only using the final model’s loss.

4 Dataset size, privacy, model size and accuracy

Previous work has shown that as models get more complex, they are more vulnerable to MIAs. For example, [39] demonstrate that their attack’s accuracy increases as the model size increases on standard benchmark image datasets. In Federated Learning, Li et al. [23] reported that, the larger the models, the more vulnerable they are to model memorization attacks. In their case, it was a horizontal FL architecture with the same model (ResNet) both in the server and the clients. Other works have highlighted that over-parameterized models are vulnerable to membership memorization attacks [41].

In this section, we shed further light on this topic by focusing on the privacy-accuracy trade-off in FL with respect to dataset and model size, and from the perspective of both the server and the

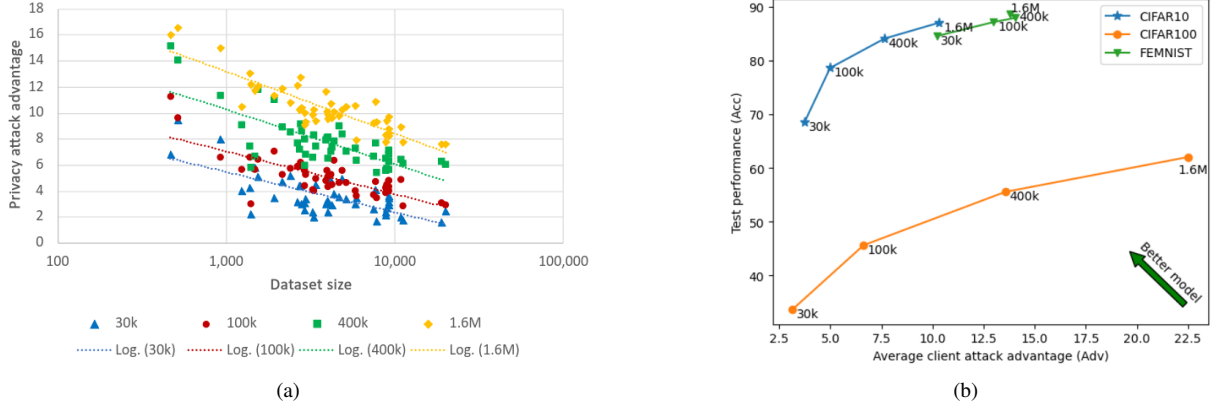


Figure 1. (a): Correlation between the privacy attack advantage for the \mathcal{Y}_{eom} attack and the dataset size from the clients’ perspective. Results for 5 repeated experiments on the CIFAR-10 dataset using the FedAvg architecture with 10 clients having different dataset sizes, resulting in 50 client models. Each dot depicts a client in one federated training and the color represents different model complexities (CNNs), characterized by the number of parameters, ranging from 30k to 1.6 million. Note the negative correlations between the size of the clients’ dataset and the attack advantage, as well as between the model’s complexity and the associated attack advantage. (b): Privacy-accuracy trade-off of the data depicted in (a) by averaging experiments across clients per model complexity. In addition to CIFAR-10, we also show the trade-off for the CIFAR-100 and FEMNIST datasets. The attacker’s advantage and test accuracy on the clients increases as the model size increases. Observations in (a) and (b) lead us to propose model-agnostic Federated Learning as a privacy-enhancing solution.

clients. Note that prior studies have only analyzed the server’s performance. We empirically show that, for a given model and an FL scenario, there is a strong negative correlation between the size of the clients’ datasets and models, and their vulnerability against a membership inference attack (\mathcal{Y}_{eom}). As previously discussed, this attack occurs on the last update the client sends to the server in round T , $\mathcal{A}_{\mathcal{Y}_{\text{eom}}}(\theta_c^T)$. We use the \mathcal{Y}_{eom} attack for this experiment as it requires significantly less computation than the other described MIAs.

We perform the experiments on the CIFAR-10 image dataset (see Section 6 for a description of the dataset) with 10 homogenous clients and a FedAvg FL architecture [28]. In FedAvg the clients train the same model as the server using their own dataset, such that the average of the clients’ model weights is an approximation of training the same model in a centralized machine with access to all client data. That is, FedAvg computes $\min_{\theta} L(\theta)$, given by: $\min_{\theta} L(\theta) =$

$$\min_{\theta} \frac{1}{|\mathbb{D}|} \sum_{c=1}^C \sum_{(x,y) \in \mathbb{D}_c} l(y, f(x, \theta)) \approx \frac{1}{C} \sum_{c=1}^C \min_{\theta_c} L_c(\theta_c, \mathbb{D}_c) \quad (2)$$

where L is the loss function in the server when having access to all the client data; l is the loss function in each client; θ and f are server model parameters and server architecture, respectively. The loss at each client $L_c(\theta_c, \mathbb{D}_c)$ is given by $\frac{1}{|\mathbb{D}_c|} \sum_{(x,y) \in \mathbb{D}_c} l(y, f(x, \theta_c))$, where C is the number of clients; and \mathbb{D}_c represents the dataset of client c such that $\mathbb{D} = \bigcup_{c=1}^C \mathbb{D}_c$ corresponds to the entire dataset.

To ensure a fair evaluation, the attacker’s knowledge dataset \mathbb{D}_{A+} for the \mathcal{Y}_{eom} ’s attack is proportionate to the size of the training dataset. Specifically, we select 1%: $|\mathbb{D}_{A+}| = \min(3, 0.01|\mathbb{D}_c|)$ for the attack on client c with dataset size $|\mathbb{D}_c|$. The attack test dataset \mathbb{D}_{MIA} contains the same number of samples from the training set as samples from outside of the training set. If the client c has less than 5,000 data samples, we test on all of the client data samples with non-member examples from the test set, so that $|\mathbb{D}_{\text{MIA}}| = 2|\mathbb{D}_c|$, otherwise it is capped at 5,000. With such a dataset setting, a simple baseline which guesses that each MIA test data point is part of the training dataset would give a 50% accuracy. We define the **attack advantage** [16] as the improvement of an attack when compared to this baseline according to: $Adv(\mathcal{A}) = 2(Acc(\mathcal{A}) - 50)$, where $Acc(\mathcal{A})$ is the accuracy of the attacker’s model.

Regarding the machine learning models, we adopt the architecture proposed in [10]. It consists of a convolutional neural network (CNN) with 4 convolutional layers and one fully connected layer at the end. We adjust the model complexity by changing the number of channels in the convolutional layers and the number of units in the last fully connected layer. We define 4 levels of model complexity and train 5 models for each level of complexity using FedAvg with class-balanced data in each client, resulting in 50 client models. The complexity of the models is measured by the number of parameters, ranging from models with 30k to models with 1.6 million parameters.

For each model complexity, we compute the Pearson correlation coefficient between the logarithm of the clients’ dataset size, $\log_{10}(|\mathbb{D}_c|)$, and the attack advantage on the clients’ final update, $Adv(\mathcal{A}_{\mathcal{Y}_{\text{eom}}}(\theta_c^T))$. Figure 1(a) visually illustrates the correlation between the client’s dataset size and the attack advantage on the models of increasing complexity on the CIFAR-10 dataset. Note that clients with less than 400 data points are not considered in the calculation as their attack performance is not consistent through runs due to having very small (< 4) attacker knowledge. Figure 1(b) depicts the privacy-accuracy trade-off by averaging experiments across clients for each model complexity on the CIFAR-10, CIFAR-100, and FEMNIST datasets. We observe strong negative correlations between the size of the clients’ dataset and the attack’s advantage; and between the clients’ model complexity and the corresponding attack’s advantage. We also observe that both the attacker’s advantage and the test accuracy on the clients increase as the model size increases.

5 Taxonomy of model-agnostic FL methods

In this section, we frame existing model-agnostic FL methods according to a novel taxonomy which allows to both compare existing methods and identify new methods to complete the taxonomy.

5.1 Formulation

In the following, we assume a model-agnostic FL architecture where both the server and clients’ models are CNNs with a different number of channels in each layer, but the same number of layers.

Table 1. Proposed taxonomy of model-agnostic FL methods by means of model compression in the clients. **a)**: FL methods with dynamic selection of the clients’ model size. All clients are assumed to hold a model of the same complexity as the server’s model. These methods are not applicable to settings where clients have data and computation constraints, as it is our case. Thus, they are beyond the scope of this paper. **b)**: FL methods where the clients have a fixed model size, which can be smaller than the server’s model size. In this case, the clients apply different strategies to select the channels from the server’s model to be used in their training. The blue font corresponds to newly proposed methods that are analyzed in section 5.4.

		Dynamic client size selection methods	
		Random	Gradient
Update	Each round		Flado [24]
	Each batch	FjORD [15]	

(a)

		Selection strategy	
		Resampled (S)	Fixed (F)
Coverage	One group (O)	OSM, OSR	HeteroFL [10], OFR
	Several groups (G)	GSR	GFM, GFR
	Unique (U)	FDropout [6]	UFR

(b)

In such a setting, a model-agnostic FL method achieves model reduction $\theta_c \subset \theta$ in client c by limiting the size of each layer in the client’s network according to the following principle: a layer represented by weight matrix $\mathbf{A}^{N \times M} \in \theta$ is reduced to size $N_c \times M_c$, where $N_c < N$ and $M_c < M$ such that every cell $a_c^{i_c, j_c}$ the reduced matrix $\mathbf{A}_c^{N_c \times M_c}$ corresponds to a cell $a^{i, j}$ in the original matrix $\mathbf{A}^{N \times M}$:

$$\forall i_c, j_c : a_c^{i_c, j_c} \in \mathbf{A}_c, \exists i, j : a^{i, j} \in \mathbf{A}, a_c^{i_c, j_c} = a^{i, j} \quad (3)$$

We introduce a taxonomy of model-agnostic FL methods reflected in Table 1. The first group of methods shown in Table 1(a) includes algorithms that *dynamically* select the size of the clients’ models but where all the clients hold models of the same size as the server. Thus, these methods define an $M_s(\cdot)$ function that determines the $N_c \times M_c^l$ dimensions of the weight matrix \mathbf{A}_c^l for each layer l in the model $f(\theta_c)$ of client c . Note that the methods in this category assume that all the clients are able to train models of size $N \times M$, but only a subset of the dimensions are selected in each round of training. Flado [24] and FjORD [15] belong to this group. Note that they are not applicable to settings where clients have data and computation constraints, as it is our case. Hence, they are out-of-the-scope of this paper.

The second group, depicted in Table 1(b) and illustrated in Figure 2, includes methods where the clients have *fixed-size* models that are typically smaller than the server’s model. As we are considering CNNs, we refer to this family of methods as *channel selection* methods. The weights of each layer in a 2D CNN are defined by an (N, M, H, W) dimensional tensor, where M and N are the input and output channels of the layer and H and W are the height and width of the kernel, respectively. For each linear layer, $\mathbf{A}^{N \times M}$ denotes its weight matrix where M and N are the input and output data dimensions [42, 20], and $a^{i, j}$ represents the kernel weights of the (i, j) position. In this case, $Ch(\cdot) : \mathbf{A}^{N \times M, l} \rightarrow \mathbf{A}_c^{N_c \times M_c, l}$ determines the mapping between the cells of the server’s weight matrix \mathbf{A}^l and client’s c smaller matrix \mathbf{A}_c^l for each layer l . Without a loss of generalization, we assume that the channels are sorted.

5.2 Channel selection in model-agnostic FL

Figure 3 further develops the taxonomy presented in Table 1(b) by adding a new dimension, yielding three dimensions.

The first dimension of the taxonomy refers to coverage, classifying the methods in three classes: *one group* (O); *several groups* (G); and *unique* (U), depending on the number of channel sets used to train in the clients with smaller models than the server’s model. In *one group*, each client selects the same set of channels. In *several groups*, clients are clustered in groups such that clients in the same group use the same set of channels (Figure 3 shows an example with 4 groups). *Unique* corresponds to federations where every client has their set of channels selected individually.

The second dimension characterizes the strategy for channel selection and defines two types: *fixed* (F) methods when the channel sets are defined at the beginning of the training, and *resampled* (S) methods when the channel sets are selected in each training round.

Finally, the third dimension divides methods into two kinds: *sub-matrix* (M) methods if the selected channels are the first or second half of the full channel list and *random* (R) methods if the channels are selected randomly.

5.3 Existing model-agnostic FL algorithms

We describe next existing model-agnostic FL methods from the perspective of our taxonomy.

1. FDropout In FDropout [6], all the clients learn a CNN with the same architecture but fewer parameters (smaller weight matrices) than the server, and the server randomly drops a fixed number of units from each client [35], mapping the sparse model to a dense, smaller network by removing the dropped weights.

While the original formulation of FDropout used the same model size in all the clients, an extended model-agnostic variation was proposed by [15] that allows clients to have different model sizes. In this variation, randomly selected cells, $a^{i, j}$ and their associated rows i and columns j are dropped from the weight matrix. The size of the client’s matrix can be set by the number of dropped rows and columns: $|Drop(N, N_c)| = N - N_c$ and $|Drop(M, M_c)| = M - M_c$, where $Drop(n, k)$ selects k elements from n randomly. Therefore, for FDropout, we have:

$$a^{i, j} \in \mathbf{A}_c : i \notin Drop(N, N_c), j \notin Drop(M, M_c). \quad (4)$$

Thus, FDropout corresponds to a USR method because each client has a different, random set of channels in each training round.

2. HeteroFL HeteroFL [10] follows a similar idea as FDropout but with two key differences when selecting the channels in the clients with smaller models than the server: 1) all the clients learn from the same portion of the server’s model; and 2) instead of randomly dropping cells, the clients always keep the top-left subset of the server’s weight matrix for each layer in the network. Thus, in HeteroFL, the weight matrix \mathbf{A}_c^l of size $N_c \times M_c$ in layer l and client c corresponds to the top-left sub-matrix of the server’s weight matrix \mathbf{A}^l of size $N \times M$:

$$\forall a_c^{i, j} \in \mathbf{A}_c, a^{i, j} \in \mathbf{A} : a_c^{i, j} = a^{i, j}, i = 1..N_c, j = 1..M_c. \quad (5)$$

According to our taxonomy, HeteroFL corresponds to an OFM method as there is only one client group with fixed channels that correspond to a sub-matrix of the server’s weight matrix.

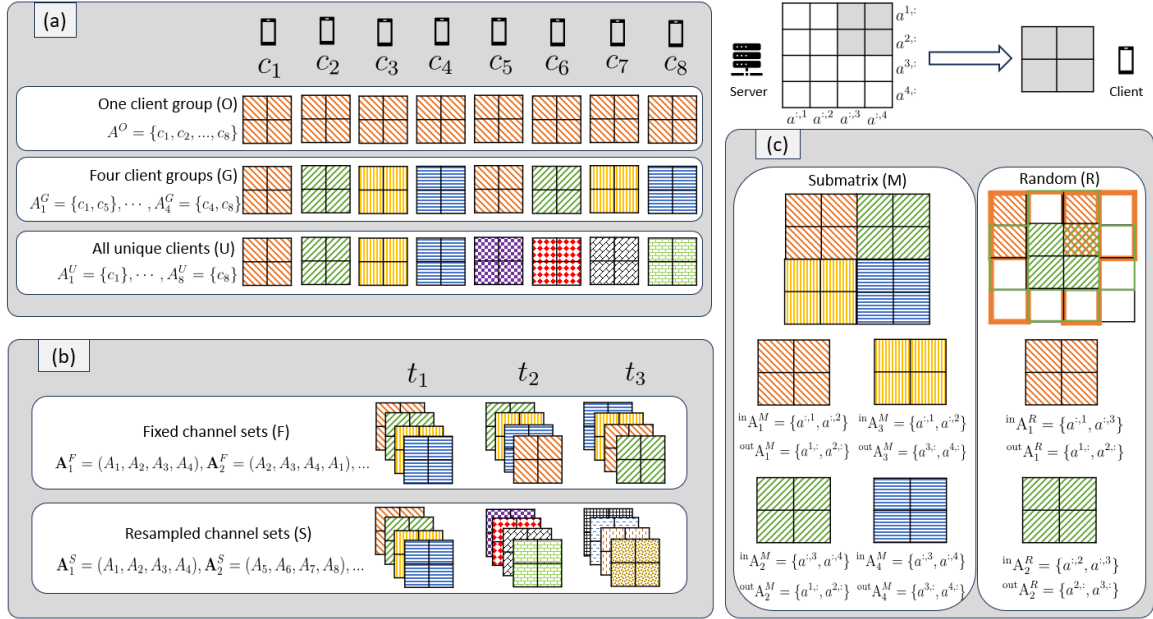


Figure 2. Taxonomy of channel selection methods for model-agnostic FL architectures with fixed model size in the clients. The server and the clients learn the same type of models (e.g. CNNs) but with different numbers of units. The clients with smaller models need to select channels from the server’s model as part of their learning process. The taxonomy considers three dimensions: **a)** Number of clients learning from the same server channels: one group (O), four groups (G), all unique clients (U); **b)** Channel group selection: fixed at the beginning of the training (F), sampled in each round (S); and **c)** Channel selection: according to a submatrix structure (M), randomly (R).

Even though both HeteroFL and FDropout are explained using the weight matrix of a layer in the model independently from other layers, in practice the input channels of layer l must be the same as the output channels of the previous layer ($l-1$) in sequential models. The FDropout implementation in [24] follows the same principle. Therefore, the input channels—columns of the weight matrix A —are inherited from the previous layer in the network, and only the output channels—rows of the weight matrix—are selected for the current layer.

5.4 Newly proposed model-agnostic FL methods

From our taxonomy, we identify seven additional model-agnostic FL methods, depending on how the clients are grouped and which portions of the server’s model are used to train the clients.

1. GFM In method GFM, instead of selecting the top-left sub-matrix of the server’s model, the clients are randomly placed in N groups. In the following, we present the example where $N=4$. Thus, the clients are assigned to one of 4 groups, O, P, Q, R . The client’s channels are selected based on their group’s policy, such that each cell from the original matrix is assigned to one cell in one of the four group.

The matrix assigned to group O is the same as the HeteroFL sub-matrix: it always selects the top-left cells of the server’s matrix. Clients in group R are assigned the bottom-right cells. The sub-matrices assigned to clients in groups O and P alternate between the bottom-left and the top-right cells. This is due to the restriction on the input-output channels. The top-right sub-matrix corresponds to selecting the second half of the input channels and the first half of the output channels. Therefore, if in layer l the client selected the top-right sub-matrix, in the next layer it has to select one of the left sub-matrices, as they are the ones with the first half of the input channels. Note that this approach can be generalized to 9, 16, ... groups, depending on the number of clients and the desired model size reduction. The cell assignment in the sub-matrices of each of the four

groups is summarized in Equation 6 below.

2. GFR Compared to GFM, the method GFR differs only in the set of channels in A_O, A_P, A_Q , and A_R . Instead of selecting the first or the last N_c and M_c channels, the output channels are selected randomly, while the input channels match the output channels of the previous layer.

$$a^{(i,j),l} \in \begin{cases} A_O, & \text{if } 1 \leq i \leq N_c, 1 \leq j \leq M_c \\ A_P, & \text{if } 1 \leq i \leq N_c, M - M_c \leq j \leq M, l \text{ odd,} \\ & \text{or } N - N_c \leq i \leq N, 1 \leq j \leq M_c, l \text{ even} \\ A_Q, & \text{if } N - N_c \leq i \leq N, 1 \leq j \leq M_c, l \text{ odd,} \\ & \text{or } 1 \leq i \leq N_c, M - M_c \leq j \leq M, l \text{ even} \\ A_R, & \text{if } N - N_c \leq i \leq N, M - M_c \leq j \leq M \end{cases} \quad (6)$$

3. GSR In GSR, the set of channels are drawn randomly for each group in every round of training.

4. OSM OSM generalizes HeteroFL by leveraging the channel sets $\{A_O, A_P, A_Q, A_R\}$ introduced in GFM, but in each training round all clients are using one of the 4 groups.

5. OFR The method OFR is a variation of HeteroFL where instead of the top-left subset of channels in the server’s weight matrix, the clients all get the same random set of channels for every round of training.

6. OSR In OSR, the set of channels are drawn randomly in every training round, but all clients use the same set.

7. UFR Finally, the method UFR has C unique sets of channels from the server’s model which are defined at the beginning of the training and clients have access to one according to a new permutation every round. Therefore, the clients receive the parameters from the same set of channels every 10 rounds in our example as we are considering a federation with 10 clients.

5.5 Privacy-accuracy trade-off

Each of the proposed methods is anticipated to provide a different privacy-accuracy trade-off, depending on how the clients are grouped and how they select the portions of the server’s matrix to use in their training. We formulate below three hypotheses in this regard that we validate empirically in our experiments.

H1: Frequency Hypothesis We hypothesize that methods where clients have access to the same set of channels more frequently perform better in terms of client model accuracy but have a worse client-level privacy. For example, in GFM the clients access the same set of channels every four rounds. Thus, compared to HeteroFL and FDropout we expect this method to yield a client privacy-performance trade-off between these two existing methods.

Based on this hypothesis we expect:

- OSR, GSR, and USR (i.e., FDropout) to be the most resilient methods against MIAs but provide the worst client accuracy as the clients receive the parameters from a new set of channels in every round. Therefore, the same set is only repeated in every $\binom{N}{N_c}$ rounds on average for client c with client channel size N_c and server channel size N .
- OFM (i.e., HeteroFL) and OFR to be the most vulnerable against MIAs but achieve high client accuracies as the clients train using the parameters of the same set of channels in every round (1 round).

H2: Similarity between the M and R categories In a CNN layer, as long as the selected input channels of layer l match the output channels of layer $l - 1$, the differences between variations M and R should be small. They differ only in the number of channels shared by client groups. We designed the sub-matrix category (M) to minimize the channel overlap between groups. Thus, we expect the models in the M and R categories to behave similarly.

H3: The differences in the privacy-accuracy trade-off between the methods decrease as the number of large clients in the federation increases The channel selection methods discussed in this paper are relevant when the majority of the clients learn smaller models than the server’s model. In fact, in cases when all the clients but one learn models of the same complexity as the server’s model, the UFR and OFR methods become the same. Therefore, we expect the impact of the channel selection strategies to be larger when the majority of clients in the federation learn smaller models than the server’s model.

We perform a comparative analysis of the proposed model-agnostic FL methods and empirically validate our hypotheses in experiments on two vision datasets, as described next.

6 Experiments

6.1 Datasets

We perform experiments on two widely used image datasets: CIFAR-10 and CIFAR-100.

CIFAR-10 [19] is a commonly used dataset both in the FL [28, 10, 15] and the MIA [39, 18] literature. It contains 60,000 images from 10 classes (50,000 images for training and validation and 10,000 images for testing).

CIFAR-100 [19] has the same number of training and testing images as CIFAR-10 but with 100 classes and 500 training images per class.

Table 2. Correlation between the performance of the 3 MIAs (Y_{eom} , LiRA, t_{MIA}) on the CIFAR-10 dataset using common metrics in MIA literature [9, 16].

	(a) AUC			(b) Adv			(c) TPR@FPR 0.1%		
	tMIA	LiRA	Yeom	tMIA	LiRA	Yeom	tMIA	LiRA	Yeom
tMIA	1.00	0.83	0.98	1.00	0.70	0.78	1.00	0.00	0.46
LiRA	0.83	1.00	0.85	0.70	1.00	0.68	0.00	1.00	0.02
Yeom	0.98	0.85	1.00	0.78	0.68	1.00	0.46	0.02	1.00

For CIFAR-10 and CIFAR-100, we use a class-wise balanced, but client-wise weighted-distribution. We generate a data distribution using the Dirichlet distribution $Dir(\alpha)$ once, and apply the same split for each class. This ensures that each client has the same number of images from each class while they have different dataset sizes. The IID-ness of the data is controlled by the $\alpha \in (0, \infty)$ value of the Dirichlet distribution: the larger the α , the closer the allocation of training data to the uniform distribution and hence the closer to an IID scenario. Using $\alpha = 0.85$ this distribution generates clients with dataset size typically ranging from 1,000 to 10,000 samples. We apply *random crop* and *random flip* augmentations.

6.2 Methodology

Machine learning model Given the nature of the data (images), we use a sequential CNN architecture, with convolutional, batch normalization and fully connected layers with trainable weights following [10]. We control the model complexity by changing the number of channels in the convolutional layers and the number of units in the final fully connected layer. In our experiments, we increase the complexity by factors of 2: each increase in the level of model complexity entails doubling the input and output channel sizes in each inner convolutional layer and the number of units in the final fully connected layer. A detailed description of the model architecture is available in the supplementary material (section 1).

Experimental setup In all experiments we define a FL architecture with 10 clients which are trained with the Adam optimizer, a learning rate of 0.001 for one local epoch, a batch size of 128, and 150 rounds of FL. Experiments are repeated 3 times and we report mean values. The server learns a *large* model, which corresponds to a CNN network with 100k parameters. The clients learn a model with either the same complexity as the server’s model or one complexity level below with 30k parameters (*small* model).

All models are built in PyTorch [31] with the Flower federated framework [4]. FL clients are simulated in parallel on 2 AMD EPYC 7643 48-Core CPUs with 252GB RAM. Our code is available at <https://github.com/negedng/ma-fl-mia>

Privacy performance metrics of the MIAs Measuring privacy by means of the vulnerability of the models against membership inference attacks is a common practice in the literature [16, 9]. In the following experiments, we use the AUC (area-under-ROC-curve) averaged over the 3 different MIAs. To motivate this decision, we compared the performance of the 3 attacks using three different performance metrics (AUC, attack advantage and TPR@FPR 0.1%), depicted in Table 2. As can be observed in the Table, we report AUC because this metric shows the largest correlation across MIAs, ranging between 0.83 and 0.98. We therefore report the AUC averaged over the three attacks (t_{MIA} , LiRA, and Y_{eom}) as the metric to measure the model’s privacy against these attacks.

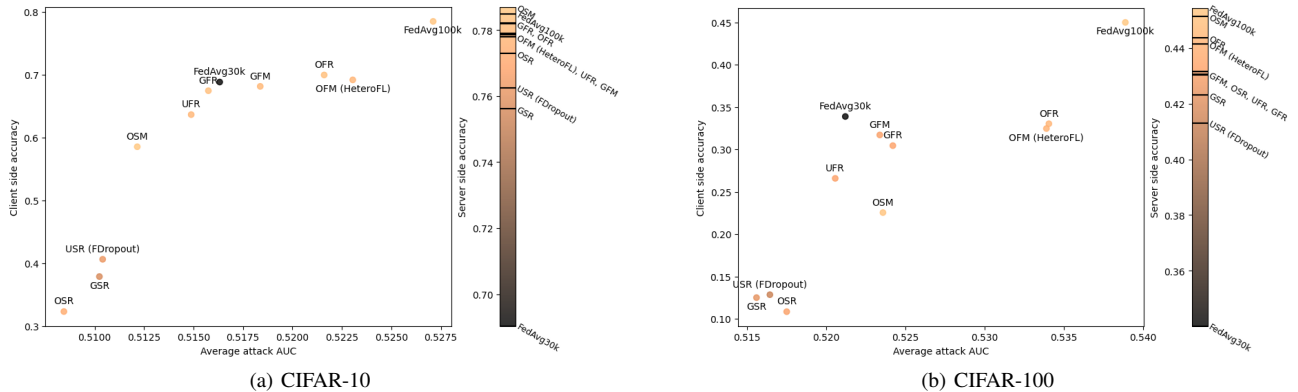


Figure 3. Experiments to measure the client-side accuracy, server-side accuracy and the client’s privacy. MIA vulnerability averaged over the 3 attacks (\mathcal{Y}_{eom} , \mathcal{L}_{IRA} , \mathcal{t}_{MIA}). All model-agnostic FL architectures have 2 clients with large models and 8 clients with small models. FedAvg30k and FedAvg100k are the baselines with 10 small (30k parameters) and 10 large (100k parameters) clients respectively.

6.3 Results

We train the 9 model-agnostic channel selection methods in a FL architecture with 10 clients, of which 2, 5, or 8 clients learn small models and the rest learn models of the same complexity as the server’s model. Clients with a smaller dataset size are selected first to learn smaller models. We also train two FedAvg baselines where the server and all the clients learn models with the large and the reduced model sizes. This results in training 29 FL models for each data distribution.

Each client is subject to the 3 previously described MIAs. For \mathcal{L}_{IRA} and \mathcal{t}_{MIA} , the auxiliary dataset is drawn from the data of the rest of the clients $\mathcal{D}_a^c = \{\mathcal{D}_1, \dots, \mathcal{D}_C\} \setminus \mathcal{D}_c$. We use the same shadow models to attack models from the same experiment. We train 16 shadow models for \mathcal{L}_{IRA} and use 25 distill epochs for \mathcal{t}_{MIA} .

Figure 3 depicts the average attack AUC of the 3 MIAs on all the model-agnostic FL channel selection methods with 2 *large* clients. Experiments on CIFAR-10 and CIFAR-100 corroborate our first hypothesis $H1$ related to the accuracy-privacy trade-off. From a client perspective, methods GFM and GFR achieve similar results to the FedAvg30k baseline with small models, yet, they outperform FedAvg30k on the server-side accuracy (77.89% and 78.19% over 69.04% for CIFAR-10 and 43.05% and 43.17% over 34.01% for CIFAR-100). Furthermore, their privacy compared to HeteroFL is better by 0.5 – 1.0% AUC with very similar levels of client accuracy. FDropout, and the GSR and OSR methods perform well in terms of client privacy, but their client accuracy is significantly lower when compared to the rest of the methods.

Supporting our $H2$ hypothesis, methods GFR and GFM, and methods OFR and OFM yield similar results in all three measures on the two datasets, with OFM (HeteroFL) and OFR on CIFAR-100 being the closest with differences of only 0.2%, 0.6%, and 0.02% on the server accuracy, client accuracy, and attack AUC, respectively.

Interestingly, while the OSM method performs as expected on the client side, it outperforms every method on its server-side accuracy. Therefore, it provides the best server accuracy-client privacy trade-off from all the studied model-agnostic FL methods.

Impact of the number of clients with small model complexity

The choice of the investigated methods has impact when the majority of the clients that join the federation learn models that are smaller than the server’s model. Table 3 summarizes the difference in performance between the best and the worse performing methods when 2, 5, and 8 out of 10 clients learn models of the same model complexity as the server’s model. The gap in performance between the best and

worst performing models in a federation with 2 *large* clients and a federation with 8 *large* clients is **3x** for the server-side accuracy and attack AUC, and over **6x** for the client-side accuracy. This supports hypothesis $H3$.

Non-IID data We study the impact of non-IID data (non independent and identically distributed) using the Federated EMNIST or FEMNIST [7] dataset, which is an image dataset of hand-written characters. It consists of 62 classes with a long-tail data distribution. In its federated version, the images are distributed by the ID of the writer whose handwriting they are. Following the official sub-sampling method, we select 20% of the data, keeping only writers with at least 300 samples and splitting into train-test datasets where the test dataset corresponds to images by unseen. This results in approximately 165 writers in the train set. We distribute the data among 10 clients following the standard practice in the literature [38]. We do not apply data augmentation on this dataset.

Table 3. Differences in performance between the best and worse performing methods in federations with 2, 5, and 8 *large* clients. As the ratio of clients with the same model size as the server increases, the differences in performance between the channel selection algorithms decreases corroborating our third hypothesis.

%	CIFAR-10			CIFAR-100		
	2	5	8	2	5	8
Server Acc	$\Delta 3.09$ (75.61-78.70)	$\Delta 0.56$ (78.44-79.00)	$\Delta 0.72$ (78.38-79.10)	$\Delta 3.82$ (41.31-45.13)	$\Delta 1.13$ (44.57-45.70)	$\Delta 1.69$ (44.85-46.54)
Client Acc	$\Delta 37.65$ (32.30-69.95)	$\Delta 20.61$ (51.41-72.02)	$\Delta 6.63$ (67.32-73.96)	$\Delta 22.18$ (10.85-33.02)	$\Delta 11.88$ (24.27-36.08)	$\Delta 3.25$ (37.03-40.06)
Attack Avg. AUC	$\Delta 1.52$ (50.78-52.30)	$\Delta 0.87$ (51.69-52.56)	$\Delta 0.65$ (52.40-53.06)	$\Delta 1.85$ (51.56-53.41)	$\Delta 1.32$ (52.61-53.85)	$\Delta 0.99$ (52.91-53.90)

While the hypotheses formulated in Section 5.5 hold for the non-IID experiments on the client-side, the server-side accuracy significantly drops when using model-agnostic methods: 2.2 points for FL with 2 *large* clients, and 0.9 points for 5 *large* clients. Furthermore, the FedAvg100k baseline outperforms several model-agnostic methods regarding client privacy. These results shed light on limitations of channel selection methods in model-agnostic FL, and suggest that further research is needed to develop novel model-agnostic FL methods that consider the spurious correlations within the clients [43]. The supplementary material (section 4) contains more details about the experiments with non-IID data.

7 Conclusion

In this paper, we have empirically shown that privacy in federated learning can be enhanced by means of a model-agnostic approach. We have proposed a novel taxonomy that not only frames existing approaches but also has enabled us to propose 7 new methods. In extensive empirical evaluations with the CIFAR-10 and CIFAR-100 datasets, we demonstrate that the proposed new FL algorithms can outperform existing methods regarding their trade-off between server-side accuracy, client-side accuracy and client performance. Our work supports the hypothesis that model-agnostic FL can significantly bolster privacy protections while maintaining or even improving performance metrics across distributed systems. By establishing a comprehensive taxonomy and introducing novel methodologies, we pave the way for enhanced privacy of sensitive data within federated learning environments.

Acknowledgements

G.D.N. and N.O. have been partially supported by funding received at the ELLIS Unit Alicante Foundation by the European Commission under the Horizon Europe Programme - Grant Agreement 101120237 - ELIAS, and a nominal grant from the Regional Government of Valencia in Spain (Convenio Singular signed with Generalitat Valenciana, Conselleria de Innovación, Industria, Comercio y Turismo, Dirección General de Innovación). G.D.N. is also funded by a grant by the Banco Sabadell Foundation. G.D.N. acknowledges travel support from the European Union's Horizon 2020 research and innovation programme under ELISE Grant Agreement No 951847. G.D.N. and N.Q. have been supported in part by a European Research Council (ERC) Starting Grant for the project "Bayesian Models and Algorithms for Fairness and Transparency", funded under the European Union's Horizon 2020 Framework Programme (Grant Agreement 851538).

References

- [1] M. Abadi, A. Chu, I. Goodfellow, H. B. McMahan, I. Mironov, K. Talwar, and L. Zhang. Deep learning with differential privacy. In *Proceedings of the 2016 ACM SIGSAC conference on computer and communications security, CCS '16*, page 308–318, New York, NY, USA, 2016. Association for Computing Machinery.
- [2] K. Arikumar, S. B. Prathiba, M. Alazab, T. R. Gadekallu, S. Pandya, J. M. Khan, and R. S. Moorthy. Fl-pmi: Federated learning-based person movement identification through wearable devices in smart healthcare systems. *Sensors*, 22(4):1377, 2022.
- [3] D. Bernau, J. Robl, P. W. Grassal, S. Schneider, and F. Kerschbaum. Comparing local and central differential privacy using membership inference attacks. In *Data and Applications Security and Privacy XXXV: 35th Annual IFIP WG 11.3 Conference, DBSec 2021, Calgary, Canada, July 19–20, 2021, Proceedings*, pages 22–42. Springer, 2021.
- [4] D. J. Beutel, T. Topal, A. Mathur, X. Qiu, J. Fernandez-Marques, Y. Gao, L. Sani, H. L. Kwing, T. Parcollet, P. P. d. Gusmão, and N. D. Lane. Flower: A friendly federated learning research framework. *arXiv preprint arXiv:2007.14390*, 2020.
- [5] D. Byrd and A. Polychroniadou. Differentially private secure multi-party computation for federated learning in financial applications. In *Proceedings of the First ACM International Conference on AI in Finance*, pages 1–9, 2020.
- [6] S. Caldas, J. Konečný, H. B. McMahan, and A. Talwalkar. Expanding the reach of federated learning by reducing client resource requirements. *arXiv preprint arXiv:1812.07210*, 2018.
- [7] S. Caldas, S. M. K. Duddu, P. Wu, T. Li, J. Konečný, H. B. McMahan, V. Smith, and A. Talwalkar. Leaf: A benchmark for federated settings. In *Workshop on Federated Learning for Data Privacy and Confidentiality*, 2019.
- [8] N. Carlini, C. Liu, Ú. Erlingsson, J. Kos, and D. Song. The secret sharer: Evaluating and testing unintended memorization in neural networks. In *USENIX Security Symposium*, volume 267, 2019.
- [9] N. Carlini, S. Chien, M. Nasr, S. Song, A. Terzis, and F. Tramer. Membership inference attacks from first principles. In *2022 IEEE Symposium on Security and Privacy (SP)*, pages 1897–1914. IEEE, 2022.
- [10] E. Diao, J. Ding, and V. Tarokh. Hetero{fl}: Computation and communication efficient federated learning for heterogeneous clients. In *International Conference on Learning Representations*, 2021.
- [11] C. Dwork. Differential privacy. In *International colloquium on automata, languages, and programming*, pages 1–12. Springer, 2006.
- [12] M. Fredrikson, S. Jha, and T. Ristenpart. Model inversion attacks that exploit confidence information and basic countermeasures. In *Proceedings of the 22nd ACM SIGSAC conference on computer and communications security*, pages 1322–1333, 2015.
- [13] Y. Gu, Y. Bai, and S. Xu. Cs-mia: Membership inference attack based on prediction confidence series in federated learning. *Journal of Information Security and Applications*, 67:103201, 2022.
- [14] N. Homer, S. Szelinger, M. Redman, D. Duggan, W. Tembe, J. Muehling, J. V. Pearson, D. A. Stephan, S. F. Nelson, and D. W. Craig. Resolving individuals contributing trace amounts of dna to highly complex mixtures using high-density snp genotyping microarrays. *PLOS Genetics*, 4:1–9, 08 2008.
- [15] S. Horvath, S. Laskaridis, M. Almeida, I. Leontiadis, S. Venieris, and N. Lane. Fjord: Fair and accurate federated learning under heterogeneous targets with ordered dropout. *Advances in Neural Information Processing Systems*, 34:12876–12889, 2021.
- [16] H. Hu, Z. Salicic, L. Sun, G. Dobbie, P. S. Yu, and X. Zhang. Membership inference attacks on machine learning: A survey. *ACM Computing Surveys (CSUR)*, 54(11s):1–37, 2022.
- [17] B. Jayaraman, L. Wang, K. Knipmeyer, Q. Gu, and D. Evans. Revisiting membership inference under realistic assumptions. *Proceedings on Privacy Enhancing Technologies*, 2021(2), 2021.
- [18] Y. Kaya and T. Dumitras. When does data augmentation help with membership inference attacks? In M. Meila and T. Zhang, editors, *Proceedings of the 38th International Conference on Machine Learning*, volume 139 of *Proceedings of Machine Learning Research*, pages 5345–5355. PMLR, 18–24 Jul 2021.
- [19] A. Krizhevsky. Learning multiple layers of features from tiny images. Master's thesis, University of Tront, 2009.
- [20] Y. LeCun, B. Boser, J. S. Denker, D. Henderson, R. E. Howard, W. Hubbard, and L. D. Jackel. Backpropagation applied to handwritten zip code recognition. *Neural computation*, 1(4):541–551, 1989.
- [21] A. Li, J. Sun, P. Li, Y. Pu, H. Li, and Y. Chen. Hermes: an efficient federated learning framework for heterogeneous mobile clients. In *Proceedings of the 27th Annual International Conference on Mobile Computing and Networking*, pages 420–437, 2021.
- [22] D. Li and J. Wang. Fedmd: Heterogenous federated learning via model distillation. In *NeurIPS Workshop on Federated Learning for Data Privacy and Confidentiality*, 2019.
- [23] Z. Li, L. Wang, G. Chen, Z. Zhang, M. Shafiq, and Z. Gu. E2egi: End-to-end gradient inversion in federated learning. *IEEE Journal of Biomedical and Health Informatics*, 2022.
- [24] D. Liao, X. Gao, Y. Zhao, and C.-Z. Xu. Adaptive channel sparsity for federated learning under system heterogeneity. In *Proceedings of the IEEE/CVF Conference on Computer Vision and Pattern Recognition*, pages 20432–20441, 2023.
- [25] R. Liu, F. Wu, C. Wu, Y. Wang, L. Lyu, H. Chen, and X. Xie. No one left behind: Inclusive federated learning over heterogeneous devices. In *Proceedings of the 28th ACM SIGKDD Conference on Knowledge Discovery and Data Mining*, pages 3398–3406, 2022.
- [26] Y. Liu, Z. Zhao, M. Backes, and Y. Zhang. Membership inference attacks by exploiting loss trajectory. In *Proceedings of the 2022 ACM SIGSAC Conference on Computer and Communications Security*, pages 2085–2098, 2022.
- [27] G. Long, Y. Tan, J. Jiang, and C. Zhang. Federated learning for open banking. In *Federated Learning: Privacy and Incentive*, pages 240–254. Springer, 2020.
- [28] B. McMahan, E. Moore, D. Ramage, S. Hampson, and B. A. y Arcas. Communication-efficient learning of deep networks from decentralized data. In *Artificial intelligence and statistics*, pages 1273–1282. PMLR, 2017.
- [29] G. D. Németh, M. A. Lozano, N. Quadrianto, and N. M. Oliver. A snapshot of the frontiers of client selection in federated learning. *Transactions on Machine Learning Research*, 2022.
- [30] A. Oprea and A. Vassilev. Adversarial machine learning: A taxonomy and terminology of attacks and mitigations. Technical report, National Institute of Standards and Technology US Department of Commerce, 2023.
- [31] A. Paszke, S. Gross, S. Chintala, G. Chanan, E. Yang, Z. DeVito, Z. Lin, A. Desmaison, L. Antiga, and A. Lerer. Automatic differentiation in

- pytorch. In *NIPS 2017 Workshop Autodiff Submission*, 2017.
- [32] M. Shin, C. Hwang, J. Kim, J. Park, M. Bennis, and S.-L. Kim. Xor mixup: Privacy-preserving data augmentation for one-shot federated learning. *arXiv preprint arXiv:2006.05148*, 2020.
 - [33] R. Shokri, M. Stronati, C. Song, and V. Shmatikov. Membership inference attacks against machine learning models. In *2017 IEEE symposium on security and privacy (SP)*, pages 3–18. IEEE, 2017.
 - [34] L. Song, R. Shokri, and P. Mittal. Membership inference attacks against adversarially robust deep learning models. In *2019 IEEE Security and Privacy Workshops (SPW)*, pages 50–56. IEEE, 2019.
 - [35] N. Srivastava, G. Hinton, A. Krizhevsky, I. Sutskever, and R. Salakhutdinov. Dropout: a simple way to prevent neural networks from overfitting. *The journal of machine learning research*, 15(1):1929–1958, 2014.
 - [36] J. Tan, D. LeJeune, B. Mason, H. Javadi, and R. G. Baraniuk. A blessing of dimensionality in membership inference through regularization. In *International Conference on Artificial Intelligence and Statistics*, pages 10968–10993. PMLR, 2023.
 - [37] J. Xu, B. S. Glicksberg, C. Su, P. Walker, J. Bian, and F. Wang. Federated learning for healthcare informatics. *Journal of Healthcare Informatics Research*, 5:1–19, 2021.
 - [38] L. Yang, C. Beliard, and D. Rossi. Heterogeneous data-aware federated learning. *IJCAI 2020 Federated Learning Workshop*, 2020.
 - [39] S. Yeom, I. Giacomelli, M. Fredrikson, and S. Jha. Privacy risk in machine learning: Analyzing the connection to overfitting. In *2018 IEEE 31st computer security foundations symposium (CSF)*, pages 268–282. IEEE, 2018.
 - [40] C. Yun-Hin, J. Zhihan, D. Jing, and N. C.-H. Edith. Fedin: Federated intermediate layers learning for model heterogeneity. *arXiv preprint arXiv:2304.00759*, 2023.
 - [41] C. Zhang, Z. Xiaoman, E. Sothiawat, Y. Xu, P. Liu, L. Zhen, and Y. Liu. Generative gradient inversion via over-parameterized networks in federated learning. In *Proceedings of the IEEE/CVF International Conference on Computer Vision*, pages 5126–5135, 2023.
 - [42] W. Zhang, J. Tanida, K. Itoh, and Y. Ichioka. Shift-invariant pattern recognition neural network and its optical architecture. In *Proceedings of annual conference of the Japan Society of Applied Physics*, volume 564. Montreal, CA, 1988.
 - [43] C. Zhou, X. Ma, P. Michel, and G. Neubig. Examining and combating spurious features under distribution shift. In *International Conference on Machine Learning*, pages 12857–12867. PMLR, 2021.

Supplementary Material

Balancing Privacy and Accuracy with Model Complexity in Model-Agnostic Federated Learning

1 Machine learning model description

The model in all our experiments is a Convolutional Neural Network, similar to the models reported in related work [3]. The layers with weight matrices consist of 2D convolutional layers with a (N, M, H, W) 4-dimensional matrix, where the first two dimensions N and M correspond the output and input channels and the rest are the convolutional kernels. From a model-agnostic perspective, N and M are the dimensions that change when the clients in the federation learn models of different size than the server’s model whereas H and W are the same as in the server. In the PyTorch implementation, the bias of the convolutional layers has a separate (N) 1-dimensional matrix. When a subset of N_c^l output channels is selected for a client c and convolutional layer l , its bias shares the same N_c^l out of N^l output channels.

After the convolutional layers in the model architecture, there are BatchNorm normalization layers with (N) 1-dimensional weight matrices with bias. Note that the BatchNorm layer $l + 2$ after convolutional layer l has the same $N_c^{l+2} = N_c^l$ channels selected. The Scaler layer adapted from HeteroFL [3] scales its input with respect to the model-agnostic compression rate. For $r_c = \frac{N_c}{N} = \frac{M_c}{M}$, the Scaler follows:

$$f_{\text{Scaler}}(x) = \frac{1}{r_c}x. \quad (7)$$

Finally, there is a linear layer l with weight matrix (N, M) and bias with weight matrix size (N) . Each client c shares the same N_c^l output channels on this linear layer.

The complexity of the model is controlled with parameter u . Each input and output dimension of the weight matrix is a multiple of u . The model complexity levels used in this paper –namely 30k, 100k, 400k, and 1.6M– correspond to u values of 8, 16, 32, and 64, respectively. Figure 4 illustrates the model architecture for a generic u and an example with $u = 16$.

2 Membership Inference Attacks

2.1 Y_{eom} attack

In this attack [5], the attacker chooses a global threshold ν , and selects every data instance with a loss lower than the threshold as a member of the training dataset. To determine the threshold, the adversary can use a subset of known data instances, called attacker’s knowledge: $\mathbb{D}_{A+} \subset \mathbb{D}_g$ for samples from the training data and $\mathbb{D}_{A-} \not\subset \mathbb{D}_g$. During the attack, the instance’s loss is compared with the average loss from the known training data points to infer the membership of data point (\mathbf{x}, y) to the training dataset:

$$\mathcal{A}_{Y_{\text{eom}}}(\hat{y}, (\mathbf{x}, y)) = \begin{cases} 1, & \text{if } l(y, \hat{y}) < \nu \\ 0, & \text{otherwise.} \end{cases},$$

$$\nu = \frac{1}{|\mathbb{D}_{A+}|} \sum_{(\mathbf{x}', y') \in \mathbb{D}_{A+}} l(y', f(\mathbf{x}', \theta)) \quad (8)$$

Fix model architecture		Changing size			
		u=16		u	
Input (32x32x3)	(HxW)	N	M	N	M
Conv2D	3x3	16	3	u	3
Scaler					
BatchNorm		16		u	
ReLU					
MaxPool2D					
Conv2D	3x3	32	16	2u	u
Scaler					
BatchNorm		32		2u	
ReLU					
MaxPool2D					
Conv2D	3x3	64	32	4u	2u
Scaler					
BatchNorm		64		4u	
ReLU					
MaxPool2D					
Conv2D	3x3	128	64	8u	4u
Scaler					
BatchNorm		128		8u	
ReLU					
GlobalAveragePool2D					
Flatten					
Dense		10	128	10	8u
Output (10)					

Figure 4. Model architecture and sizes of the weight matrices depending on the model complexity, controlled by the parameter u . Layer names and constant parameter dimensions on the left, varying dimensions on the right.

2.2 LiRA attack

We use the offline version of the LiRA attack of [6]. In this attack, the attacker has an auxiliary dataset \mathbb{D}_a and train shadow models $M_{sw}(f, \mathbb{D}_{sw})$ on random subsets of this dataset $\mathbb{D}_{sw} \subset \mathbb{D}_a$.

For a given data instance (\mathbf{x}, y) , the algorithm calculates the logit of the confidence score for each shadow model $\phi(M_{sw}(\mathbf{x}, y))$. To the set of confidence scores $\{\phi(M_1), \dots, \phi(M_k)\}_{(\mathbf{x}, y)}$, it fits a Gaussian distribution $\mathcal{N}(\mu, \sigma^2)$, and the membership probability is $1 - Pr[\mathcal{N}(\mu, \sigma^2) > \phi(M(\mathbf{x}, y))]$.

$$\mathcal{A}_{\text{LiRA}}(\hat{y}, (\mathbf{x}, y), \mathbb{D}_a) = \begin{cases} 1, & \text{if } 1 - Pr[\mathcal{N}(\mu, \sigma^2) > \phi(\hat{y}, y)] < \nu \\ 0, & \text{otherwise.} \end{cases} \quad (9)$$

2.3 tMIA attack

In this attack [7], the membership value of a data point is determined by the loss trajectory of the data instance. The hypothesis is that if we take a snapshot of the loss of a data point with respect to the model after each training epoch, this trajectory is different for member and non-member instances. However, the loss trajectories are not accessible when querying only the final model in a black-box MIA. Therefore, the proposed method uses knowledge distillation to simulate the training.

Let's denote the target model as $M_{tg}^0(f, \mathbb{D}_g)$. First, the attack trains a shadow model $M_{sw}^0(f, \mathbb{D}_{sw}^+)$ with dataset $(\mathbb{D}_{sw}^+, \mathbb{D}_{sw}^-) \subset \mathbb{D}_a$. Second, it distills a model to both the target (M_{tg}^d) and the shadow (M_{sw}^d) models using a distill dataset $\mathbb{D}_{dl} \subset \mathbb{D}_a$, saving the models $M_{tg}^1, \dots, M_{tg}^d$ and $M_{sw}^1, \dots, M_{sw}^d$ after each training epoch. The loss trajectory of a data instance (\mathbf{x}, y) is the loss of that data point on each model during the distillation process $\lambda_*^{(\mathbf{x}, y)} = \{l_*^0, l_*^1, \dots, l_*^d\}_{(\mathbf{x}, y)}$, where $l_*^i = L(M_*^i(\mathbf{x}, y))$, $* \in \{tg, sw\}$.

The next step is to build an attack model M_A that expects a loss trajectory $\lambda^{(\mathbf{x}, y)}$ as an input and determines whether the data instance (\mathbf{x}, y) is a member. To train this model, the method uses the loss trajectory on the shadow model with data instances from the shadow dataset: $\lambda_{sw}^{(\mathbf{x}, y)}$, $\forall (\mathbf{x}, y) \in \{\mathbb{D}_{sw}^+ \cup \mathbb{D}_{sw}^-\}$.

Finally, in inference time it predicts membership of a data point (\mathbf{x}, y) using the loss trajectory of the target model distillation steps $\lambda_{tg}^{(\mathbf{x}, y)}$ and the attacker model (M_A).

$$\mathcal{A}_{\text{tMIA}}(\hat{y}, (\mathbf{x}, y), \mathbb{D}_a) = \begin{cases} 1, & \text{if } M_A(\lambda_{tg}^{(\mathbf{x}, y)}) > \nu \\ 0, & \text{otherwise.} \end{cases} \quad (10)$$

3 Input-output channel dependency

In section 5.3 we present FDropout [3] and HeteroFL [1] according to their original descriptions, which suggest that the channels of a layer l can be dropped independently from the previous and following channels. However, after extensive experiments, we observed that the client models train significantly better if the selected output channels of a convolutional layer are *the same* as the input channels of the following convolutional layer. In the FDropout adaptation of [4] the same principled is adopted: layer l only drops output channels randomly, while the selection of the input channels is inherited from the previous convolutional layer. The pseudocode in [2] suggests that their implementation follows the original layer-independent dropout and their results show that FDropout

performs badly compared to other techniques: while the Simple Ensemble Averaging method reached the 70% accuracy of the baseline FedAvg on FEMNIST dataset, the presented implementation of FDropout only reached 60%. In table 4, we compare FDropout (USR) and GFR with input and output channels dropped independently and with layer-wise coupling with respect to the previous and following layer. The results show that the client side accuracy for the layer-wise methods outperforms their independent counterpart by 16% for FDropout and 7% for GFR. Based on these results we conclude that the layer-wise dependency is necessary to achieve competitive results and follow this principle in our other experiments.

Additionally, Section 1 in this supplementary material describes how the BatchNorm layers in our implementation have the same channels dropped as the previous convolutional layers.

Table 4. Input-output channels selected independently and with respect to the previous layers in the CNN. FDropout (USR) and GFR experiments on CIFAR-10 with 2 large clients out of 10 clients in total, repeated 3 times. Client-side performance is significantly better when the channel selection is structured layer-wise compared to their independent counterparts. Privacy evaluated with Yeom attack.

Name	Server		Client average	
	Acc \uparrow	Adv \downarrow	Acc \uparrow	Adv \downarrow
USR independent	75.44 σ 1.75	2.57 σ 1.62	23.56 σ 0.29	1.74 σ 0.44
USR layerwise	76.38 σ 1.36	2.45 σ 1.34	39.99 σ 1.11	2.32 σ 1.52
GFR independent	76.41 σ 1.73	2.87 σ 0.78	55.82 σ 1.61	3.00 σ 0.50
GFR layerwise	77.11 σ 1.52	3.34 σ 0.98	62.80 σ 1.43	3.20 σ 0.24

4 Detailed experimental results

4.1 Model size vs attack advantage

Table 5 shows the Pearson correlation coefficient between the client dataset sizes and their vulnerability against client-side Yeom membership inference attacks. Numbers correspond to running experiments 5 times in a federation with 10 clients. Clients with less than 400 data samples are excluded from the analysis, resulting in the exclusion of 3 clients in the 5 runs with the CIFAR-10 and CIFAR-100 datasets. All values in the table exceed the critical value of non-significant correlation for the given sample size.

Table 5. Pearson correlation coefficient of dataset size and attack advantage for different models per class balanced heterogeneous data distribution.

Model size per class	balanced	heterogeneous	data	distribution
CIFAR-10	-0.62	-0.65	-0.57	-0.87
CIFAR-100	-0.54	-0.70	-0.85	-0.90
FEMNIST	-0.71	-0.65	-0.63	-0.75

4.2 Attacks on FEMNIST dataset

Figure 5 depicts the performance of the 9 model-agnostic FL methods on the FEMNIST dataset for a federation with 2 and 5 large (100k parameters) clients and the same experimental setup as that described in the main paper.

In the case of a federation with 2 large clients (Figure Figure 5(a)), we observe significant differences in the server's performance when compared to the results obtained with the CIFAR-10 and CIFAR-100 datasets. Contrary to the CIFAR-x datasets, methods GFR, OSR, OFM, and OFR underperform when compared to the FedAvg30k baseline.

In a federation with 5 large clients (Figure Figure 5(b)), the server-side results are more similar to those obtained on the CIFAR-x datasets: method OSM yields the best server-side accuracy and all the

methods outperform `FedAvg30k`. Interestingly and contrary to the behavior on the CIFAR-x datasets, `FDropout` is competitive with the other methods on its server-side accuracy yet yields poor client-side accuracy.

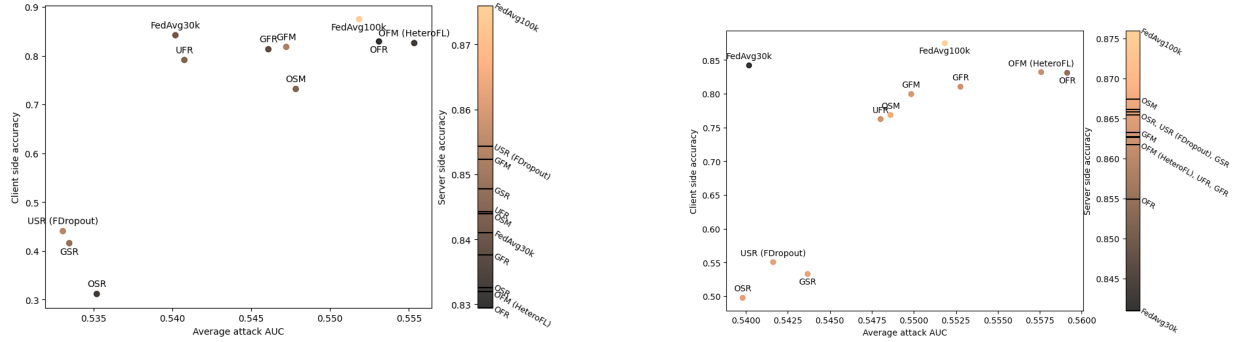
In future work we plan to further study the behavior of model-agnostic FL methods on non-IDD data. We speculate that these differences in behavior might be due to spurious correlations, which are inexistent in the CIFAR-x datasets yet present in the FEMNIST dataset, as the writer’s style might be correlated to certain classes and clients [8].

4.3 Attacks on CIFAR-10 and CIFAR-100 datasets

Results on the two CIFAR datasets are summarized in the main paper in included in detail in Table 7 and Table 8.

References

- [1] Sebastian Caldas, Jakub Konečný, H. Brendan McMahan, and Ameet Talwalkar. Expanding the reach of federated learning by reducing client resource requirements, 2018
- [2] Gary Cheng, Zachary Charles, Zachary Garrett, and Keith Rush. Does federated dropout actually work? In *Proceedings of the IEEE/CVF Conference on Computer Vision and Pattern Recognition*, pages 3387–3395, 2022.
- [3] Enmao Diao, Jie Ding, and Vahid Tarokh. Hetero{fl}: Computation and communication efficient federated learning for heterogeneous clients. In *International Conference on Learning Representations*, 2021.
- [4] Dongping Liao, Xitong Gao, Yiren Zhao, and Cheng-Zhong Xu. Adaptive channel sparsity for federated learning under system heterogeneity. In *Proceedings of the IEEE/CVF Conference on Computer Vision and Pattern Recognition*, pages 20432–20441, 2023
- [5] S. Yeom, I. Giacomelli, M. Fredrikson, and S. Jha. Privacy risk in machine learning: Analyzing the connection to overfitting. In *2018 IEEE 31st computer security foundations symposium (CSF)*, pages 268–282. IEEE, 2018.
- [6] N. Carlini, S. Chien, M. Nasr, S. Song, A. Terzis, and F. Tramèr. Membership inference attacks from first principles. In *2022 IEEE Symposium on Security and Privacy (SP)*, pages 1897–1914. IEEE, 2022.
- [7] Y. Liu, Z. Zhao, M. Backes, and Y. Zhang. Membership inference attacks by exploiting loss trajectory. In *Proceedings of the 2022 ACM SIGSAC Conference on Computer and Communications Security*, pages 2085–2098, 2022.
- [8] C. Zhou, X. Ma, P. Michel, and G. Neubig. Examining and combating spurious features under distribution shift. In *International Conference on Machine Learning*, pages 12857–12867. PMLR, 2021.



(a) Performance of the 9 model-agnostic FL methods and baselines on the FEMNIST dataset with 2 *large* (100k parameters) clients. The server-side accuracy of several model-agnostic FL methods is inferior to FedAvg30k’s accuracy. Contrary to the results obtained on the CIFAR-x datasets, FDropout is the model-agnostic FL method with the best server-side accuracy.

(b) Performance of the 9 model-agnostic FL methods and baselines on the FEMNIST with 5 *large* (100k parameters) and 5 *small* (30k parameters) clients. The non-IID dataset requires more *large* clients in the federation to outperform the FedAvg30k baseline on the server-side accuracy. The most privacy-sensitive model-agnostic approaches, such as OFM (HeteroFL) yield worse client accuracy-privacy trade-off than the FedAvg100k baseline in this non-IID setting.

Figure 5. Performance of the 9 model-agnostic methods and baselines on the FEMNIST dataset with 2 and 5 *large* (100k parameters) clients. These results suggest that more sophisticated model-agnostic approaches that take into account spurious correlations beyond channel selection strategies are needed.

No. of <i>large</i>	Method name	↑ Server		↓ AUC %				↓ Attack Adv %				↓ TPR% at 0.1% FPR			
		Acc %	Acc %	tMIA	LiRA	Yeom	Avg	tMIA	LiRA	Yeom	Avg	tMIA	LiRA	Yeom	Avg
10	FedAvg100k	87.60	87.49	56.41	53.17	55.98	55.18	7.67	5.20	7.26	6.71	0.27	0.25	0.15	0.22
	FedAvg30k	84.10	84.20	55.45	51.20	55.41	54.02	6.86	2.26	7.01	5.38	0.15	0.14	0.16	0.15
2	GFM	85.23	81.80	56.27	51.72	56.18	54.72	8.29	2.69	7.66	6.21	0.22	0.16	0.13	0.17
2	GFR	83.76	81.32	55.95	51.78	56.10	54.61	7.56	2.39	7.21	5.72	0.19	0.20	0.15	0.18
2	GSR	84.78	41.59	54.80	50.28	54.95	53.35	5.89	0.73	5.67	4.10	0.16	0.07	0.10	0.11
2	OFM (HeteroFL)	83.19	82.59	57.24	52.62	56.74	55.53	9.21	4.02	8.50	7.24	0.24	0.16	0.13	0.18
2	OFR	82.95	82.92	56.93	52.51	56.49	55.31	8.68	3.09	8.17	6.65	0.28	0.11	0.11	0.17
2	OSM	84.39	73.18	56.47	51.55	56.33	54.78	8.60	2.35	8.39	6.44	0.22	0.15	0.08	0.15
2	OSR	83.26	31.17	54.93	50.49	55.14	53.52	6.26	1.06	6.02	4.45	0.17	0.12	0.09	0.13
2	UFR	84.42	79.12	55.53	51.15	55.54	54.08	7.13	1.95	6.44	5.17	0.16	0.13	0.13	0.14
2	USR (FDropout)	85.43	44.05	54.78	50.18	54.95	53.31	6.20	0.69	5.76	4.22	0.17	0.10	0.10	0.12
5	GFM	86.33	79.94	56.55	52.03	56.37	54.98	9.23	2.86	7.21	6.44	0.25	0.13	0.05	0.14
5	GFR	86.27	81.04	56.86	52.33	56.64	55.28	8.52	3.65	8.08	6.75	0.26	0.15	0.08	0.16
5	GSR	86.61	53.28	55.62	51.64	55.84	54.37	6.95	2.36	6.71	5.34	0.26	0.14	0.07	0.16
5	OFM (HeteroFL)	86.18	83.21	57.19	52.86	57.23	55.76	8.88	4.46	8.70	7.35	0.28	0.19	0.05	0.17
5	OFR	85.49	83.10	57.60	52.99	57.15	55.91	9.28	5.24	8.71	7.74	0.27	0.20	0.06	0.18
5	OSM	86.74	76.85	56.20	52.16	56.22	54.86	7.42	2.98	7.57	5.99	0.20	0.16	0.06	0.14
5	OSR	86.54	49.75	55.35	51.31	55.28	53.98	6.91	1.68	6.33	4.97	0.23	0.11	0.07	0.14
5	UFR	86.27	76.24	56.24	51.99	56.18	54.80	8.09	3.11	8.06	6.42	0.30	0.12	0.07	0.16
5	USR (FDropout)	86.58	55.04	55.52	51.38	55.59	54.16	6.44	2.10	6.75	5.10	0.25	0.17	0.05	0.16
8	GFM	87.38	80.89	56.29	52.72	56.63	55.21	8.37	4.38	7.50	6.75	0.27	0.20	0.13	0.20
8	GFR	87.12	80.74	56.86	53.06	56.79	55.57	8.98	4.73	8.52	7.41	0.23	0.20	0.07	0.17
8	GSR	87.64	73.19	56.46	52.61	56.47	55.18	8.50	3.71	7.16	6.45	0.32	0.17	0.10	0.20
8	OFM (HeteroFL)	87.04	83.93	57.97	53.41	57.73	56.37	8.96	4.22	8.62	7.27	0.27	0.22	0.05	0.18
8	OFR	86.47	83.44	57.44	53.23	57.47	56.05	9.32	4.79	8.40	7.51	0.32	0.25	0.07	0.21
8	OSM	87.33	79.80	56.77	52.66	56.87	55.43	9.18	3.84	7.58	6.87	0.28	0.13	0.12	0.18
8	OSR	87.27	72.63	56.33	52.62	56.45	55.13	8.39	3.86	7.20	6.48	0.30	0.20	0.16	0.22
8	UFR	87.05	76.97	56.86	52.91	56.82	55.53	9.03	4.32	8.86	7.40	0.31	0.20	0.10	0.20
8	USR (FDropout)	86.99	72.76	56.40	52.63	56.50	55.18	8.07	4.63	7.70	6.80	0.30	0.15	0.12	0.19

Table 6. Detailed results on the FEMNIST dataset. Experiments averaged over 3 runs

No. of large	Method name	↑ Server Acc %	↑ Client Acc %	↓ AUC %				↓ Attack Adv %				↓ TPR% at 0.1% FPR			
				tMIA	LiRA	Yeom	Avg	tMIA	LiRA	Yeom	Avg	tMIA	LiRA	Yeom	Avg
10	FedAvg100k	78.48	78.47	53.62	51.77	52.62	52.67	3.94	2.49	3.03	3.16	0.16	0.08	0.14	0.13
0	FedAvg30k	69.04	68.82	52.17	50.83	51.81	51.60	2.11	0.69	1.66	1.49	0.09	0.09	0.09	0.09
2	GFM	77.89	68.13	52.54	50.84	51.98	51.79	3.01	0.67	2.04	1.91	0.09	0.10	0.12	0.10
2	GFR	78.19	67.44	52.17	50.67	51.73	51.53	1.89	0.59	1.53	1.34	0.10	0.08	0.14	0.11
2	GSR	75.61	37.87	51.63	50.09	51.19	50.97	1.87	0.03	1.79	1.23	0.09	0.07	0.07	0.08
2	OFM (HeteroFL)	77.79	69.17	53.30	51.13	52.47	52.30	3.22	1.46	3.04	2.57	0.10	0.06	0.12	0.10
2	OFR	78.22	69.95	53.30	50.94	52.28	52.17	2.60	0.68	1.95	1.74	0.14	0.08	0.11	0.11
2	OSM	78.70	58.52	51.73	50.48	51.40	51.20	2.16	1.19	2.38	1.91	0.10	0.08	0.07	0.08
2	OSR	77.29	32.30	51.06	50.32	50.97	50.78	1.05	0.23	1.10	0.79	0.10	0.10	0.10	0.11
2	UFR	77.87	63.64	52.03	50.58	51.78	51.46	2.29	0.39	2.23	1.64	0.10	0.08	0.11	0.10
2	USR (FDropout)	76.26	40.61	51.52	50.27	51.19	51.00	2.48	0.16	1.23	1.29	0.08	0.11	0.10	0.10
5	GFM	78.89	68.23	53.04	50.89	52.19	52.04	4.11	1.11	2.66	2.62	0.12	0.10	0.09	0.10
5	GFR	78.95	68.92	52.58	50.76	51.92	51.75	2.55	1.14	1.87	1.85	0.12	0.06	0.10	0.09
5	GSR	78.50	52.09	52.49	50.89	51.82	51.73	3.12	0.76	1.92	1.93	0.12	0.08	0.09	0.10
5	OFM (HeteroFL)	78.69	71.00	53.55	51.38	52.77	52.56	3.66	1.87	2.66	2.73	0.13	0.10	0.12	0.12
5	OFR	78.84	72.02	53.76	50.93	52.68	52.46	4.24	0.70	3.60	2.85	0.10	0.07	0.07	0.08
5	OSM	79.00	66.22	52.72	51.10	51.94	51.92	3.38	1.59	1.47	2.15	0.10	0.08	0.13	0.10
5	OSR	78.86	51.41	52.64	51.23	51.89	51.92	3.41	1.55	2.68	2.55	0.12	0.10	0.08	0.10
5	UFR	78.83	64.68	52.56	51.04	51.87	51.83	2.65	1.01	2.05	1.90	0.12	0.10	0.08	0.10
5	USR (FDropout)	78.44	52.31	52.29	51.11	51.67	51.69	2.69	1.00	2.39	2.03	0.13	0.09	0.11	0.11
8	GFM	78.82	71.02	53.93	51.50	52.84	52.76	4.01	1.76	3.38	3.05	0.11	0.09	0.12	0.11
8	GFR	78.64	72.26	53.63	52.07	52.53	52.74	3.21	2.06	2.95	2.74	0.16	0.08	0.16	0.13
8	GSR	78.38	67.51	53.08	51.68	52.45	52.40	3.74	1.94	2.46	2.71	0.14	0.08	0.12	0.12
8	OFM (HeteroFL)	79.07	73.96	54.19	51.88	53.10	53.06	3.63	2.03	3.55	3.07	0.13	0.09	0.11	0.11
8	OFR	78.69	73.37	53.91	51.76	53.07	52.92	4.18	2.12	2.86	3.05	0.14	0.10	0.12	0.12
8	OSM	78.85	70.91	53.40	51.96	52.63	52.66	3.06	2.15	2.74	2.65	0.11	0.09	0.07	0.09
8	OSR	78.82	67.32	53.27	52.19	52.52	52.66	3.33	2.33	2.93	2.86	0.09	0.10	0.11	0.10
8	UFR	79.10	68.97	53.94	51.79	53.09	52.94	3.92	2.05	3.07	3.01	0.12	0.09	0.12	0.11
8	USR (FDropout)	78.87	67.74	53.55	51.95	52.72	52.74	3.65	2.18	2.58	2.80	0.13	0.11	0.13	0.13

Table 7. Detailed results on the CIFAR-10 dataset. Experiments averaged over 3 runs

No. of large	Method name	↑ Server Acc %	↑ Client Acc %	↓ AUC %				↓ Attack Adv %				↓ TPR% at 0.1% FPR			
				tMIA	LiRA	Yeom	Avg	tMIA	LiRA	Yeom	Avg	tMIA	LiRA	Yeom	Avg
10	FedAvg100k	45.44	44.98	55.20	51.82	54.65	53.89	4.64	1.60	3.10	3.11	0.13	0.10	0.06	0.10
0	FedAvg30k	34.01	33.88	52.78	50.91	52.68	52.12	2.89	0.35	1.10	1.45	0.09	0.09	0.05	0.08
2	GFM	43.05	31.70	53.11	50.96	52.95	52.34	4.24	0.50	0.88	1.88	0.10	0.08	0.11	0.10
2	GFR	43.17	30.44	53.08	51.10	53.08	52.42	4.47	1.27	2.13	2.62	0.12	0.09	0.09	0.10
2	GSR	42.32	12.51	52.12	50.68	51.89	51.56	2.24	0.99	1.08	1.43	0.10	0.07	0.10	0.09
2	OFM (HeteroFL)	44.14	32.46	54.71	51.15	54.31	53.39	4.07	0.95	3.04	2.69	0.17	0.10	0.07	0.11
2	OFR	44.36	33.02	54.62	51.33	54.28	53.41	6.11	1.50	2.43	3.35	0.10	0.07	0.06	0.08
2	OSM	45.13	22.54	53.06	51.05	52.97	52.36	3.94	0.92	1.70	2.19	0.10	0.09	0.09	0.09
2	OSR	43.05	10.85	52.28	50.87	52.11	51.75	2.86	0.75	0.98	1.53	0.11	0.08	0.14	0.11
2	UFR	43.16	26.58	52.66	50.79	52.73	52.06	2.68	-0.23	1.29	1.25	0.12	0.11	0.07	0.10
2	USR (FDropout)	41.31	12.85	52.36	50.54	52.03	51.65	3.41	1.51	1.15	2.02	0.09	0.07	0.10	0.09
5	GFM	44.57	32.49	53.92	51.38	53.59	52.96	4.82	1.49	2.50	2.94	0.10	0.07	0.11	0.10
5	GFR	45.22	32.81	54.04	51.61	53.77	53.14	4.04	0.87	1.62	2.18	0.10	0.12	0.07	0.10
5	GSR	44.84	24.20	53.56	50.81	53.24	52.54	3.98	1.41	2.09	2.49	0.10	0.10	0.07	0.09
5	OFM (HeteroFL)	44.98	35.89	55.23	51.58	54.75	53.85	4.87	1.89	3.75	3.50	0.14	0.09	0.05	0.10
5	OFR	45.39	36.08	54.82	51.34	54.50	53.55	5.11	1.06	1.31	2.49	0.11	0.08	0.09	0.09
5	OSM	45.70	29.81	53.97	51.14	53.69	52.93	4.85	-0.36	2.49	2.33	0.13	0.11	0.06	0.10
5	OSR	44.92	24.27	53.76	50.88	53.19	52.61	5.02	1.38	2.80	3.07	0.12	0.09	0.11	0.11
5	UFR	44.98	29.36	53.78	51.19	53.57	52.85	5.52	0.94	1.88	2.78	0.12	0.10	0.08	0.10
5	USR (FDropout)	45.52	24.41	53.73	51.16	53.06	52.65	4.04	1.13	1.96	2.38	0.10	0.12	0.07	0.10
8	GFM	45.55	37.98	54.49	51.56	54.01	53.35	6.14	1.91	1.02	3.02	0.12	0.09	0.07	0.09
8	GFR	46.30	38.44	54.66	51.55	54.17	53.46	5.68	1.72	1.71	3.04	0.13	0.09	0.07	0.10
8	GSR	45.65	36.81	54.03	51.74	53.68	53.15	3.72	0.56	1.27	1.85	0.14	0.09	0.07	0.10
8	OFM (HeteroFL)	44.85	39.02	54.95	51.59	54.61	53.72	6.01	2.40	2.17	3.53	0.09	0.10	0.07	0.09
8	OFR	45.71	40.06	55.18	51.63	54.88	53.90	5.09	1.37	3.17	3.21	0.11	0.15	0.10	0.12
8	OSM	45.97	37.98	54.33	51.59	54.05	53.32	4.09	1.17	1.22	2.16	0.13	0.09	0.07	0.10
8	OSR	45.30	37.03	54.00	51.68	53.68	53.12	4.56	1.97	2.73	3.09	0.19	0.10	0.12	0.13
8	UFR	46.54	38.03	54.50	51.74	54.06	53.43	5.46	1.22	2.98	3.22	0.11	0.08	0.09	0.09
8	USR (FDropout)	45.55	37.14	53.77	51.48	53.47	52.91	4.45	1.26	2.19	2.63	0.12	0.09	0.13	0.12

Table 8. Detailed results on the CIFAR-100 dataset. Experiments averaged over 3 runs